

See discussions, stats, and author profiles for this publication at: <https://www.researchgate.net/publication/231712054>

Azo Polymer Multilayer Films by Electrostatic Self-Assembly and Layer-by-Layer Post Azo Functionalization

ARTICLE in *MACROMOLECULES* · AUGUST 2000

Impact Factor: 5.8 · DOI: 10.1021/ma9921495

CITATIONS

79

READS

16

7 AUTHORS, INCLUDING:



Nirmal Viswanathan

University of Hyderabad

99 PUBLICATIONS 1,387 CITATIONS

SEE PROFILE



Jayant Kumar

University of Massachusetts Lowell

516 PUBLICATIONS 10,810 CITATIONS

SEE PROFILE



Smarak Tripathy

KIIT University

126 PUBLICATIONS 3,312 CITATIONS

SEE PROFILE

Azo Polymer Multilayer Films by Electrostatic Self-Assembly and Layer-by-Layer Post Azo Functionalization

Soo-Hyoung Lee,[†] S. Balasubramanian,[†] D. Y. Kim,[†] N. K. Viswanathan,[‡] S. Bian,[‡] J. Kumar,[‡] and S. K. Tripathy^{*,†}

Center for Advanced Materials, Departments of Chemistry and Physics, University of Massachusetts Lowell, Lowell, Massachusetts 01854

Received December 27, 1999; Revised Manuscript Received June 8, 2000

ABSTRACT: This work focuses on the development of a novel method for molecular level assembly and processing of multilayer azo polymer films. Poly(acrylic acid)-based precursor anilino-functional polymer was first synthesized and used as a polyanion. This polymer was assembled into mono- and multilayer thin films by an electrostatic layer-by-layer deposition technique in conjunction with a polycation. The aniline group in the assembled polymer layer was subsequently converted to an azobenzene chromophore by post azo coupling reaction with appropriate diazonium salts. This method provides easy control of film thickness and well-ordered chromophore structure in the multilayer. Second harmonic generation was observed in all multilayer films, indicating acentric organization of the chromophores synthesized in the multilayered films. The second harmonic intensity and film thickness are dependent on the assembly conditions (pH, etc.) of the polyions. The post-functionalized azo polymer layers were further modulated by light-driven mass transport.

Introduction

Fabrication of ultrathin polymeric films continues to be of significant interest in diverse areas of materials research including nonlinear optical (NLO) thin film devices,^{1,2} sensors,^{3,4} specialty coatings,⁵ polymeric light-emitting diodes,⁶ and bioapplications, among others.^{7,8} Electrostatic layer-by-layer (ELBL) self-assembly (SA) by alternately dipping substrates into dilute solutions of cationic and anionic polyelectrolytes has recently emerged as a simple, versatile, and effective technique for fabrication of ultrathin organic multilayer films.^{9–14} This approach provides several advantages: it is a simple, inexpensive, and environmentally friendly process (all water-based systems) which provides easy control over the thickness of the thin film at the molecular-level and long-term stability in molecular dimensions.¹⁵ In addition, it facilitates the incorporation of a variety of functional groups or macromolecules, such as conjugated polymers,¹² photoluminescent polymers,¹⁶ and groups that can undergo chemical coupling reactions¹⁷ and photochemical reactions¹⁸ into a thin film, with a well-defined structure, for a number of different applications.

Incorporation of photoresponsive azo chromophores can provide the ELBL SA films with additional interesting properties such as optically induced orientation and NLO properties. Our group and others have reported that the noncentrosymmetric ordering of chromophores, which is essential for second-order NLO properties, could be established in electrostatically self-assembled films.^{19–24} To date, a number of fundamental approaches to control the film structure, chromophore ordering, thickness, and surface properties of multilayer films have been established in the ELBL SA process.^{25–27}

Decher and co-workers have shown that the thickness of the adsorbed layers in ELBL SA process could be fine-tuned at the molecular level through ionic strength

adjustments of the dipping solution (controlling the degree of functional group ionization by pH adjustments).²⁸ Yoo et al. have demonstrated that the layer thickness and surface properties, such as wettability, of multilayer thin films fabricated from bilayers of the weak polyelectrolytes such as poly(acrylic acid) and poly(allylamine) were systematically varied by simply controlling the pH of the dipping solutions in the ELBL SA process.²⁹

Assembly and ordering of azo chromophores through chemical bond formation has been carried out by several researchers to establish better chromophore ordering in SA films in the past. Marks and co-workers treated glass substrates with a reactive trichlorosilane derivative, which can be further reacted with pyridine-based azo NLO chromophores. Improved chromophore ordering was reported in multilayer films fabricated using this process.³⁰ Katz and co-workers used zirconium phosphate/phosphate coordinate bonding to form multilayers of polar azo dyes through a sequence of surface phosphorylation, zirconation, and dye adsorption, thus resulting in a relatively large second harmonic generation (SHG) value.³¹

Therefore, these results suggest that processing parameters such as pH and chemical bond formation in the multilayers play an important role in determining the film thickness and chromophore ordering. Judicious combination of these chemistries and the assembly process can significantly expand the functional properties of the films and provide local molecular structure control. In the present work, the electrolytic behavior and excellent solubility of the polyions over a broad pH range are utilized to gain easy control over film thickness during the ELBL process. Subsequently, azo groups were directly incorporated into the precursor polymer by a convenient post azo coupling reaction on the multilayer films. This ELBL deposition and post azo functionalization combination provides a rapid and easy method of incorporating well-ordered azo chromophores in the polyion surface in the multilayer film structures.

[†] Department of Chemistry.

[‡] Department of Physics.

The effects of charge density in the polymer chains on the film thickness and chromophore ordering were investigated in these ELBL SA films over a broad range of pH values. The synthesis, characterization, multilayer fabrication, and unique optical properties such as SHG, photoinduced birefringence (PIB), and surface relief grating (SRG) formation are reported.

Experimental Section

Materials. The reagents and solvents used in the synthesis of the precursor and azo polymer were purchased from Aldrich Chemical Co. and used without further purification. The glass slides used as substrates for multilayer fabrication were purchased from VWR Scientific. The reagent used for cleaning the glass slides, Chem-solv cleaner, was obtained from Mallinckrodt. Water from a Milli-Q system was used in the multilayer fabrication process. The resistivity of the water used was higher than 18.2 M Ω ·cm, and the total organic content was less than 10 ppb.

Synthesis of Precursor Polymer (PAA-AN). The polymer (PAA-AN) was synthesized through modification of poly(acrylic acid) (PAA, MW = 2000 g/mol). A solution of 1,1'-carbonyldiimidazole (2.5 g, 15 mmol) and catalytic amount of 1,8-diazabicyclo[5.4.0]undec-7-ene in 10 mL of *N,N*-dimethylformamide (DMF) was added to a solution of poly(acrylic acid) (2.0 g, 28 mmol) in 70 mL of DMF. After stirring the light yellow solution at 25 °C until the evolution of carbon dioxide subsided, a solution of *N*-ethylanol ethanol (2.5 g, 15 mmol) in 5 mL of DMF was added, and the light yellow solution was stirred at 25 °C for 24 h. The solution was concentrated under reduced pressure to remove most of the solvent, and the concentrated solution was subsequently diluted with chloroform. The chloroform solution was poured with vigorous stirring into ether to precipitate the copolymer. The light yellow solid was extensively washed with ether and hexane and dried in a vacuum oven for 24 h at 25 °C.

Multilayer Fabrication. Slide glasses (25 × 75 mm) were hydrophilized with 1% Chem-solv solution in deionized water (DI water) under ultrasonication for use as substrates.³² This treatment generates negative charges on the surface due to partial hydrolysis. After 3 h, the slides were rinsed twice with DI water in an ultrasonicator for 30 min.

Commercially available poly(diallyldimethylammonium chloride) (PDAC) as a polycation and poly(acrylic acid)-based precursor polymer (PAA-AN) as the polyanion were used in the multilayer fabrication. Post azo functionalization by coupling reaction with the diazonium salt was directly accomplished on the polyanion surface after each polyanion layer was adsorbed. PAA-AN (10 mM) and PDAC (10 mM) aqueous solutions in different pH range (5–11) were prepared and filtered with 0.45 μ m syringe filters before use. Aqueous solution of the diazonium salt, (4-nitrobenzenediazonium tetrafluoroborate), of the same concentration was prepared and kept in an ice bath maintained at 0–5 °C.

The ELBL deposition process was carried out in three steps. In the first step, hydrophilized glass slides were immersed in PDAC solution for 10 min at room temperature and washed with DI water, adjusted to the same pH for 5 min. After the deposition and washing steps, the slides were dried with a stream of nitrogen. In the second step, the substrates with a single layer of PDAC were immersed into the PAA-AN solution for 10 min and subsequently followed by washing and drying procedures. This produces a PDAC/PAA-AN bilayer film. In the third dipping step, the surface of precursor polymer (PAA-AN) layer was azo functionalized by dipping the slides into the diazonium salt solution for 10 min, generating the azo polymer layer (PAA-AZ 1), followed by washing and drying as described earlier. This dipping sequence was iterated to build up multilayer films which consisted of 10 bilayer films made under different pH conditions of PDAC/PAA-AN solutions.

Synthesis of Azo Polymer (PAA-AZ 2). The azo group was introduced into the precursor polymer (PAA-AN) in the bulk as well to compare properties between an ELBL post azo

functionalized SA film and a spin-coated film of the azobenzene polymer. A solution of diazonium salt (0.7108 g, 3 mmol) in DMF was added dropwise into a solution of precursor polymer (PAA-AN) (0.6984 g, 2.4 mmol) in DMF maintained at 0–5 °C. After the solution was stirred at 0 °C for 12 h, the mixture was poured into water under agitation while adding a few drops of hydrochloric acid. The precipitated polymer was collected by filtration and washed with excess of water until the wash solution was neutral. The polymer was further purified by extracting repeatedly with chloroform. The solid was dried under vacuum for 24 h at 25 °C. This azo polymer was spin-coated from 1,4-dioxane solution onto glass slides to form good optical quality thin films.

Characterization. UV-vis absorption spectra were recorded using a GBC UV/vis 916 spectrophotometer. NMR spectra were taken on a Bruker ARX-250 spectrometer operating at 250 MHz. Glass transition temperature was determined using a TA Instruments differential scanning calorimeter model DSC 2910 at a heating rate of 10 °C/min.

The second-order NLO coefficients (d_{33}) of ELBL post functionalized SA films were measured by the second harmonic generation method. A horizontally polarized Q-switched Nd:YAG laser (20 Hz, 10 ns, 20 mJ at 1064 nm) was used as the fundamental beam. The sample was mounted on a rotation stage to measure the SHG intensity at different incident angles. The fundamental frequency was blocked with an appropriate filter, and the SHG signal generated from the sample was detected by a photomultiplier tube (PMT). The detected signal was averaged over 300 pulses using a boxcar integrator. By comparing the SHG intensity from the sample with that from the quartz standard (d_{11} is 0.5 pm/V), the d coefficients of the sample were determined. The refractive index and thickness of the self-assembled films are obtained using an ellipsometer (AutoEL-III, Rudolph Research, USA) and Dektak profilometer.

The formation of the holographic SRG was investigated by using a two-beam interference setup.³³ Two beams that are split from a continuous wave (CW) argon ion laser at $\lambda = 488$ nm are incident on the sample. In the sample plane, the interference between the two laser beams form a periodically modulated intensity pattern. The periodicity of the grating pattern is set at about 1.5 μ m. The two beams are p-polarized and have approximately equal intensities (~ 150 mW/cm²). The formation of SRG was monitored by detecting its first-order diffraction from an unpolarized He–Ne laser beam at $\lambda = 633$ nm. The SRG images were obtained by scanning the sample using an atomic force microscopy (AFM, Cp, Park Scientific, Sunnyvale, CA). The AFM was operated in the contact mode using a SiN cantilever.

The photoinduced birefringence (PIB) of the ELBL SA film was measured by the method described below. A 0.29 μ m thick sample was placed between two crossed polarizers (P and A) in the path of a He–Ne laser beam at 633 nm, which is far from the absorption band of the sample film. A CW laser beam at 488 nm (from an argon ion laser), which is in the trans absorption band, was incident normally upon the sample and intersect the He–Ne probe laser beam with an angle less than 10°. The polarization direction of the pump laser makes a $\pm 45^\circ$ angle with respect to the two polarization directions of the two polarizers. The intensity of the pump laser was 85 mW/cm². A birefringence Δn that was induced by the 488 nm pump laser was calculated from a transmission of the 633 nm probe beam through the second polarizer A. The transmitted probe beam intensity is described by³⁴

$$I_t = I_0 \sin^2(\delta/2)$$

where $\delta = 2\pi\Delta n d/\lambda$, d is the sample thickness, and λ is the probe laser wavelength. I_0 is the transmitted probe light intensity when $\delta = \pi$, and this value was experimentally obtained when the polarization orientations of the two polarizers are parallel to each other.

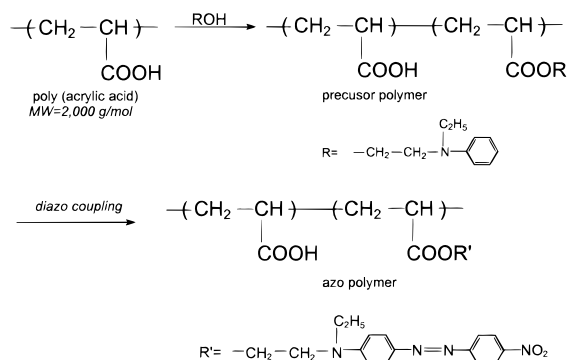


Figure 1. Synthesis scheme for a precursor polymer and an azo functionalized polymer.

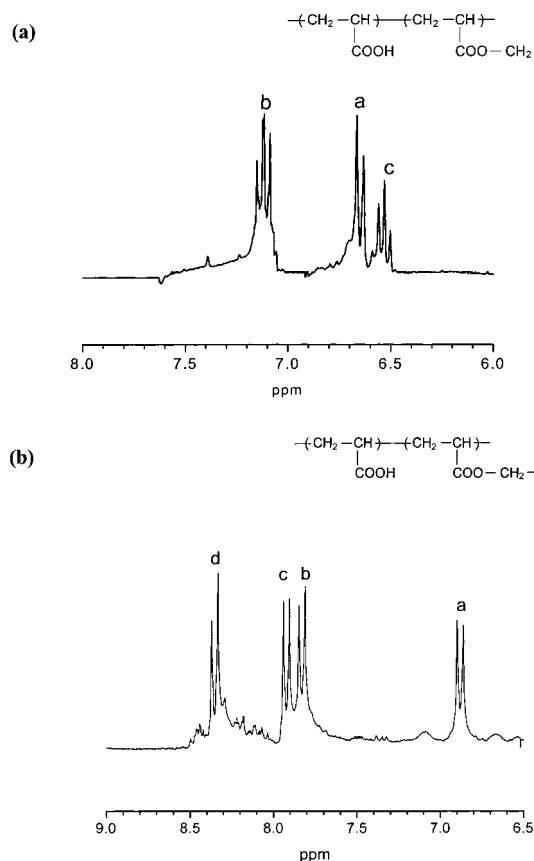


Figure 2. ^1H NMR spectra of (a) a precursor polymer (PAA-AN) and (b) an azo polymer (PAA-AZ 1) in dimethyl sulfoxide- d_6 .

Results and Discussion

Figure 1 shows the synthetic scheme for the precursor polymer and the azo polymer. Since the precursor polymer (PAA-AN) has carboxylic acid groups in its side chain, it has good solubility in water over broad pH ranges and multilayer films could be fabricated with a polycation such as PDAC in the ELBL process. This bilayer film of PDAC/PAA-AN can be subsequently azo functionalized readily with diazonium salt solution during the ELBL SA process. The materials from post azo coupling reaction were characterized using NMR spectroscopy (Figure 2). The NMR sample was prepared by scraping the multilayer film with a razor blade. Resonances at 7.12, 6.67, and 6.50 ppm correspond to chemical shifts of meta, ortho, and para protons in aniline moieties in the case of the precursor polymer (PAA-AN). After post azo coupling reaction, the reso-

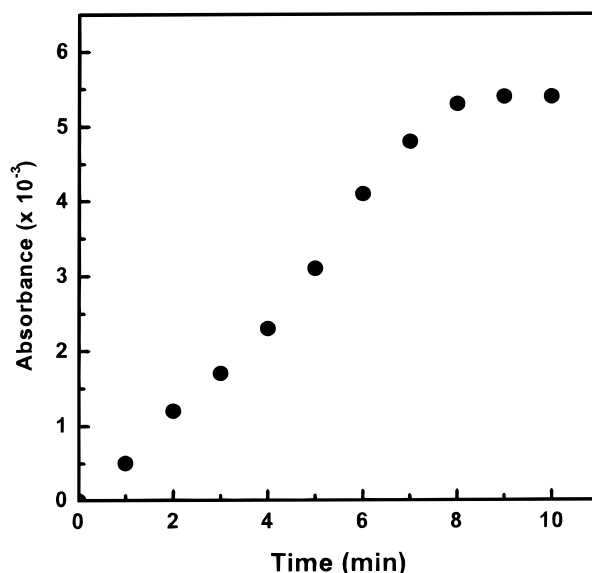


Figure 3. UV absorbance as a function of deposition time for a single bilayer film.

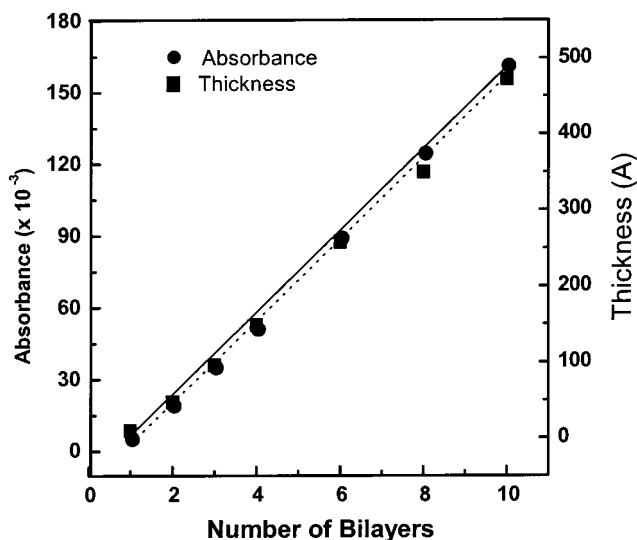


Figure 4. UV absorbance and film thickness as a function of the number of bilayers (pH of 7/7 for PDAC/PAA-AN).

nance at 6.50 ppm disappeared due to the electrophilic substitution at the para position of the aniline group. In addition, the resonances of the meta and ortho protons were shifted downfield as a result of introduction of electron-withdrawing groups and increase of conjugation length.^{35,36} Similar changes in the NMR spectrum were observed in the post azo coupling reaction for the polymer PAA-AZ 2. The T_g of the azo polymer from first heating scan of DSC was 91 $^{\circ}\text{C}$.

The ELBL deposition and post azo coupling process was monitored using UV-vis absorption spectroscopy. The absorbance of the multilayer films was similar to that of a spin-coated film of polymer PAA-AZ 2 with a λ_{max} of 475 nm. Absorbance of a single bilayer formed was measured as a function of reaction time and displayed in Figure 3. The azo coupling process saturated in about 8 min. A dipping time of 10 min in each polyion solution was used for all multilayer fabrication processes.

Figure 4 shows a linear increase in absorbance and film thickness as a function of the number of bilayers up to 10 bilayers. The linear increase in absorbance and

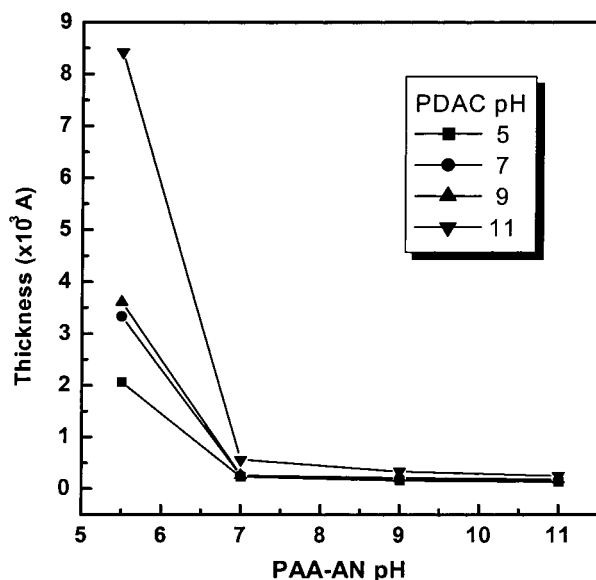


Figure 5. Thickness dependence on pH of polyanions (10-bilayer film).

film thickness indicates the uniformity of the absorption and azo coupling process.

To find the effects of polyanion solution pH on the film thickness, 10 bilayer films were fabricated under different pH conditions of polymer solutions, and the resulting film thickness was measured. Dramatic thickness changes were observed under different pH conditions of the polyanion and the polycation (Figure 5). The largest thickness value was obtained under the condition of the combination of the lowest pH of the polyanion and the highest pH of the polycation dipping solutions.³⁷

This is expected on the basis of the conformational changes of the macromolecules under different pH conditions. Polyelectrolytes possess sufficient conformational flexibility in solution.^{38,39} PAA-AN polymer has carboxylic acid groups in its side chain and becomes almost completely charged polyanion and adopts an expanded conformation only at relatively high pH. Under lower pH condition, charge density along the PAA-AN polymer chains is reduced, and the polymer molecule is expected to adopt a coiled conformation. When the polyelectrolyte molecules are adsorbed on a surface where oppositely charged ions are spread uniformly, almost fully charged polymer chains are believed to be deposited as a very thin monolayer film due to their stretched conformation. In contrast, less charged polymer chains adsorb maintaining expanded coiled conformations. Significantly thicker adsorbed layers are formed to accommodate interlayer charge compensation and these coiled conformations. Subsequent azo functionalization with diazonium salts leads to proportionately more chromophore attachment on the larger number of available functionalization sites.¹² As expected, maximum film thickness and absorbance (post functionalization) were obtained from films deposited under pH conditions in which low charge density and coiled conformation are produced (pH of 11/5.5 for PDAC/PAA-AN).

Acentric alignment and SHG in ELBL SA thin films has been reported by our group and others.^{19–24} ELBL SA of polyanions with azobenzene chromophores as side group with PDAC as the polycation was carried out. The chromophore itself contained the charged group which dictated its alignment in the ELBL deposition process.¹⁹

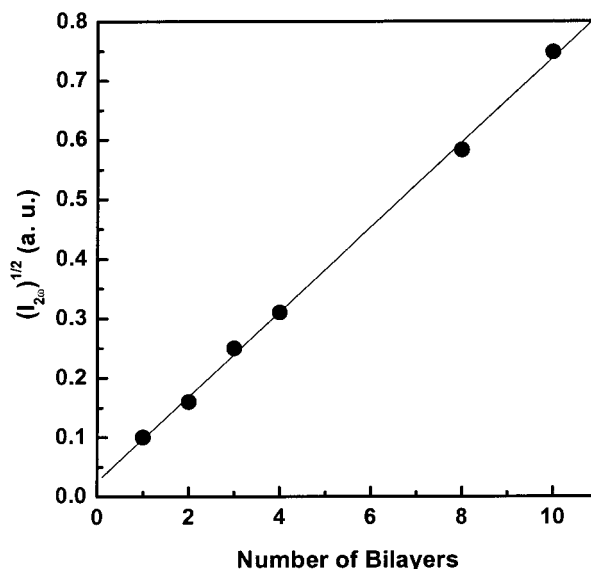


Figure 6. Square root of SHG intensity of multilayer as a function of the number of bilayers (pH of 7/7 for PDAC/PAA-AN).

In contrast in the present work azo chromophores with strong donor–acceptor substituents are introduced into the SA film post assembly and do not in themselves contain any ionic groups. SHG was observed in all ELBL post functionalized SA films of PAA-AZ 1 (prepared under different pH conditions) without any poling. Figure 6 shows the square root of SHG signal as a function of number of bilayers in the multilayer films. The plot is linear up to the 10-bilayer film investigated in this work. The second-order NLO coefficient, d_{33} , of the self-assembled films was determined to be 5.4 pm/V. The SHG intensities were measured again on the same samples after 30 days. The same SHG values were observed on all ELBL post functionalized SA films. It appears that self-organization of chromophores in these SA films has led to a thermodynamically stable system.

The dependence of SHG stability on temperature was measured in both an ELBL post azo functionalized SA film²⁰ and a spin-coated film of azo polymer PAA-AZ 2 (Figure 7). In the case of the ELBL SA film, SHG intensity decreased with increasing temperature. The decrease of SHG intensity could be a result of the randomization of chromophore ordering by thermal motions. However, some recovery of SHG signal was observed after cooling of the sample as shown in Figure 7a. We believe that the azo chromophores confined in ionic interactions formed a noncentrosymmetric ordering, and this structure is probably thermodynamically favorable in the ELBL SA films.¹⁵ In the case of the poled spin-coated films, this recovery was not detected (Figure 7b). A sudden SHG intensity drop was observed in the ELBL SA film and the poled spin-coated films at 90 and 80 °C, respectively. Several relaxation studies on the decay behavior of the second-order NLO properties of poled thick films have shown that the decay of the optical nonlinearity is closely associated with the α -relaxation temperature of the polymer.^{40,41} The SHG drop for the spin-coated film is consistent with these studies and is expected to be related to relaxation of the polymer chain near T_g . Considering that T_g of this azo polymer was measured at 91 °C, the SHG drop occurred at a temperature somewhat below T_g for the poled spin-coated films. Marturunkakul et al. have shown that the relaxation temperature in fact is somewhat lower than

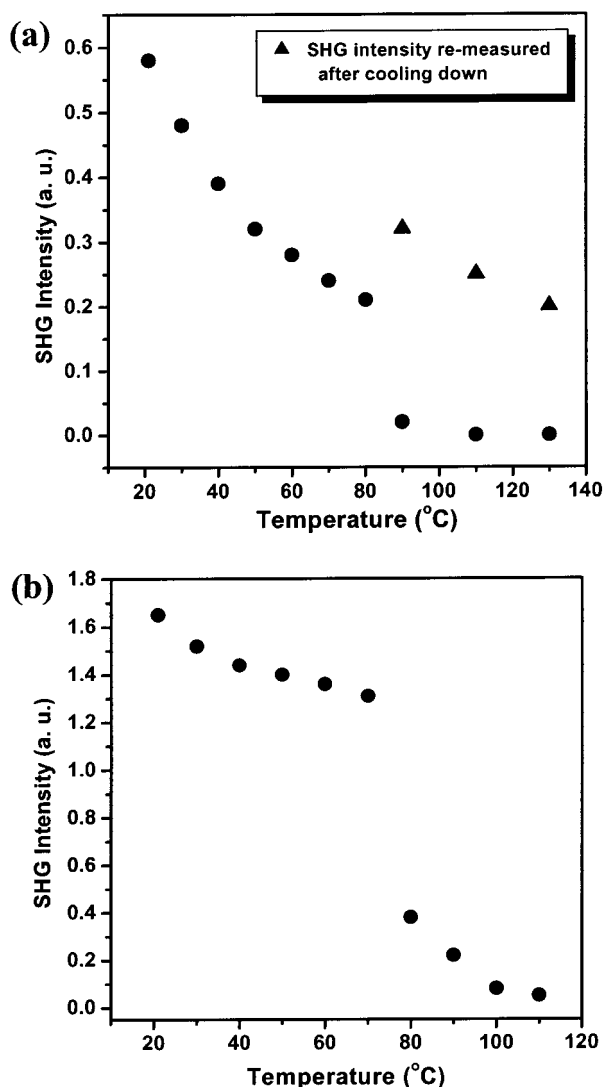


Figure 7. Temperature dependence of SHG intensity in (a) a multilayer film (10 bilayer of pH of 7/7 for PDAC/PAA-AN) and (b) a poled spin-coated film.

the bulk T_g of the polymer in the poled samples.⁴² It was suggested that, in the higher poling fields, both the NLO chromophore and the polymer backbones are in a more unstable state, and therefore relaxation occurs at a temperature lower than T_g .

The relaxation of SHG occurs at a higher temperature for the ELBL SA film and is recoverable to some extent upon cooling.¹⁵ α -Relaxation is not the relevant parameter related to the relaxation process in these thin films, and the electrostatically complexed, networked film is inherently thermodynamically more stable.^{15,20}

To find the pH dependence of SHG property, SHG intensity was measured in 10 bilayer films made from different pH conditions of the polyanion and the polycation (Figure 8). A higher SHG intensity value was obtained in lower pH of polycation and higher pH of polyanion. The SHG intensity decreased with increase of pH of PDAC and, in contrast, increased with increase of pH of PAA-AN polymer. The results imply that higher charge density polymer matrix provides better chromophore alignment. A coiled conformation of polymer chains may destroy the ordering of chromophores in these pH conditions.

The formation of optically induced birefringence was observed in all ELBL SA films. Figure 9 shows the

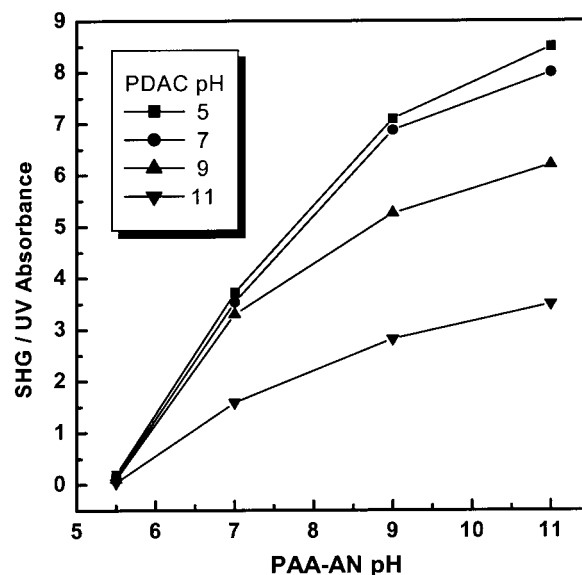


Figure 8. Dependence of SHG intensity on pH of polyanions (10-bilayer film).

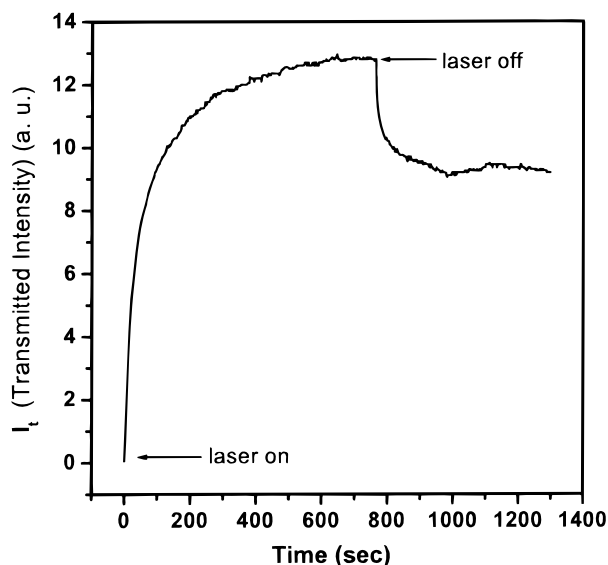


Figure 9. Transmitted light intensity monitored as a function of time for a multilayer film (10 bilayer of pH of 7/7 for PDAC/PAA-AN).

measured transmitted light intensity as a function of time on the 10-bilayer film in pH of 7/7 for PDAC/PAA-AN. The moments at which the pump lasers are switched on and off are indicated by arrows. The transmission saturates in 12 min. After switching off the pump laser the transmission exhibit a small relaxation. The birefringence Δn corresponding to the maximum transmitted intensity was 0.05. This birefringence value is almost same with that of spin-coated film (PAA-AZ 2).

Photofabrication of SRGs have been reported and extensively investigated by us in spin-coated amorphous azo polymer films. Exposing a spin-coated azo polymer films to modulated intensity pattern derived from interfering beams from an Ar ion laser at 488 nm led to the fabrication of patterned surfaces with large surface modulation.^{43,44} Details of this fabrication process and the theoretical basis for this unusual light-driven mass transport process have been presented elsewhere.^{45,46} Our earlier attempts to fabricate SRGs

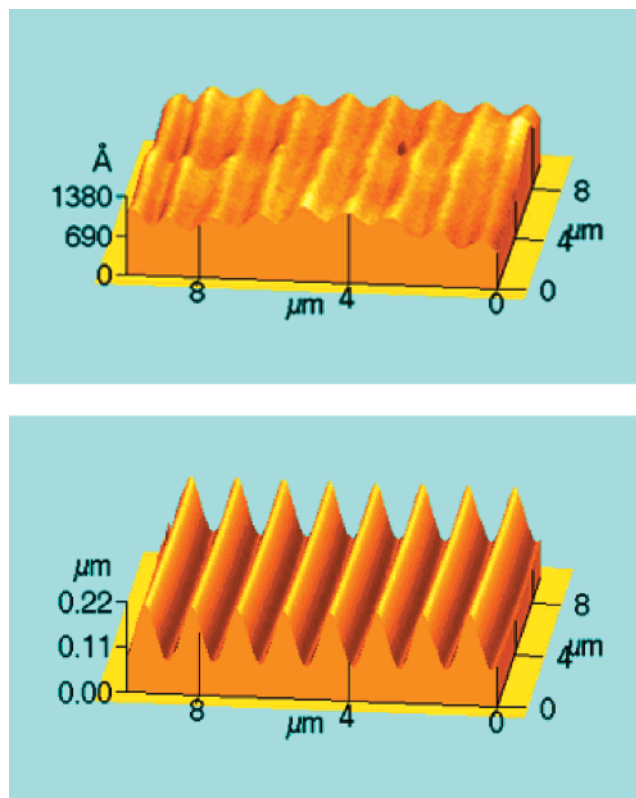


Figure 10. AFM images of SRG formation on (a, top) a multilayer film (10 bilayer of pH of 11/5.5 for PDAC/PAA-AN) and (b, bottom) a spin-coated film.

from ELBL SA thin films of polyelectrolytes containing azo chromophore were not very successful.⁴⁷ In this example, the deposited polyanion and cations were extensively charged given the pH values of the depositing solutions. Strong ionic bonds between the layers was presumed responsible for working against the light-driven mass transport process which is initiated at the sample surface. In the present work, through careful control of the pH of the polyelectrolyte solutions and modification of the deposition process (using the ELBL SA process and post azo functionalization), we were able to control and limit the extent of ionic bonds and hence inscribe SRGs on the multilayer thin films. Figure 10a shows an AFM image of SRG on the 10-bilayer film made in pH of 11/5.5 for PDAC/PAA-AN. This condition provides the film with low charge density and expanded coiled conformation for the macromolecules. A modulation depth of 250 Å was observed in this case. This modulation depth is about 3.2% of the original film thickness. Formation of SRG was not observed in ELBL SA films deposited in other pH conditions of polyions. The AFM image of SRG on the spin-coated films of polymer PAA-AZ 2 is shown in Figure 10b. Since ionic bonds do not exist in the spin-coated films, the light-driven mass transport process can be easily achieved. The modulation depth was 1300 Å for the same fluence level used for the ELBL SA film.

Conclusions

We have successfully developed a technique to fabricate the ELBL SA films in conjunction with the layer-by-layer post azo functionalization. Film thickness changed dramatically in different pH conditions of polymer solutions. Maximum thickness value was obtained under the condition of a combination of the lowest

pH for the polyanion and the highest pH for the polycation. In these conditions, the polymer chains may have a low charge density and a coiled conformation.

SHG was observed in all ELBL SA films without any poling. We believe that layer-by-layer post azo functionalization can lead to well-ordered chromophore structure in the multilayer film. SHG intensity of multilayer films increased with number of bilayers and is dependent on pH conditions. High SHG intensity was obtained under the condition of a combination of the highest pH for the polyanion and the lowest pH for the polycation in which high charge density is produced.

From the study of temperature dependence on SHG intensity, recovery of SHG intensity value was observed in the ELBL SA film upon cooling (after heating the film above 90 °C) whereas no such recovery was observed in the case of poled spin-coated film. It suggested that the noncentrosymmetric azo chromophore structure formed by ionic charge interactions in ELBL SA films leads to a thermodynamically more stable system. Finally, optically induced birefringence was observed in all ELBL SA films, and surface relief gratings could be formed on the low charge density ELBL SA film.

We believe that the easy control of film thickness and chromophore ordering in the ELBL SA process and post azo functionalization can be readily extended to a wide variety of optical applications. For example, creation of patterns on SA layers using the SRG process may lead to the generation of command surfaces for selective alignment of liquid crystal molecules.

Acknowledgment. Financial support from ONR-MURI and NSF-DMR is gratefully acknowledged. Extensive discussions with Prof. Michael F. Rubner at MIT, the MURI team, and Mr. Jaehyun Kim are acknowledged.

References and Notes

- (1) Li, D. Q.; Ratner, M. A.; Marks, T. J.; Zhang, C. H.; Yang, J.; Wong, G. K. *J. Am. Chem. Soc.* **1990**, *112*, 7389.
- (2) Katz, H. E.; Sheller, G.; Putvinski, T. M.; Shilling, M. L.; Wilson, W. L.; Chidsey, C. E. D. *Science* **1991**, *254*, 1485.
- (3) Rubinstein, I.; Steinberg, S.; Tor, Y.; Shanzer, A.; Sagiv, J. *Nature* **1988**, *332*, 426.
- (4) Rong, D.; Kim, Y. I.; Hong, H. G.; Krueger, J. S.; Mayer, J. E.; Mallouk, T. E. *Coord. Chem. Rev.* **1990**, *97*, 237.
- (5) Swalen, J. D.; Allara, D. L.; Andrade, J. D.; Chandross, E. A.; Garoff, S.; Israelachvili, J.; McCarthy, T. J.; Murray, R.; Pease, R. F.; Rabolt, J. F.; Wynne, K. J.; Yu, H. *Langmuir* **1987**, *3*, 932.
- (6) Fou, A. C.; Onitsuka, O.; Ferreira, M.; Rubner, M. F. *J. Appl. Phys.* **1996**, *79*, 7501.
- (7) Lvov, Y.; Haas, H.; Decher, G.; Mohwald, H.; Mikhaiov, A.; Mtchedlishvili, B.; Morgunova, E.; Vainshtein, B. *Langmuir* **1994**, *10*, 4232.
- (8) Lvov, Y.; Decher, G.; Sukhorukov, G. *Macromolecules* **1993**, *26*, 5396.
- (9) Cheung, J. H.; Fou, A. F.; Rubner, M. F. *Thin Solid Films* **1994**, *244*, 985.
- (10) Decher, G.; Lvov, Y.; Schmitt, J. *Thin Solid Films* **1994**, *244*, 772.
- (11) Lvov, Y.; Decher, G.; Mohwald, H. *Langmuir* **1993**, *9*, 481.
- (12) Ferreira, M.; Rubner, M. F. *Macromolecules* **1995**, *28*, 7107.
- (13) Mao, G.; Tsao, Y.; Tirrell, M.; Davis, T. H. *Langmuir* **1993**, *9*, 3461.
- (14) Saremi, F.; Tieke, B. *Adv. Mater.* **1995**, *7*, 378.
- (15) Heflin, J. R.; Figura, C.; Marciu, D.; Liu, Y.; Claus, R. O. *Appl. Phys. Lett.* **1999**, *74*, 495.
- (16) Tian, J.; Wu, C. C.; Thompson, M. E.; Sturm, J. C.; Register, R. A.; Marsella, M. J.; Swager, T. M. *Adv. Mater.* **1995**, *7*, 395.
- (17) Laschewsky, A.; Mayer, B.; Wischerhoff, E.; Arys, X.; Jonas, A.; Bertrand, P.; Delcorte, A. *Thin Solid Films* **1996**, *284–285*, 334.

- (18) Laschewsky, A.; Wischerhoff, E. *Macromol. Chem. Phys.* **1997**, *198*, 3239.
- (19) Wang, X.; Balasubramanian, S.; Li, L.; Jiang, X.; Sandaman, D. J.; Rubner, M. F.; Kumar, J.; Tripathy, S. K. *Macromol. Rapid Commun.* **1997**, *18*, 451.
- (20) Roberts, M. J.; Lindsay, G. A.; Herman, W. N.; Wynne, K. J. *J. Am. Chem. Soc.* **1998**, *120*, 11202.
- (21) Lvov, Y.; Yamada, S.; Kunitake, T. *Thin Solid Films* **1997**, *300*, 107.
- (22) Balasubramanian, S.; Wang, X.; Wang, H. C.; Yang, K.; Kumar, J.; Tripathy, S. K. *Chem. Mater.* **1998**, *10*, 1554.
- (23) Laschewsky, A.; Wischerhoff, E.; Kauranen, M.; Persoons, A. *Macromolecules* **1997**, *30*, 8304.
- (24) Lenahan, K. M.; Wang, Y.-X.; Liu, Y.; Claus, R. O.; Heflin, J. R.; Marciu, D.; Figura, C. *Adv. Mater.* **1998**, *10*, 853.
- (25) Decher, G. *Science* **1997**, *277*, 1232.
- (26) Hoogeveen, N. G.; Cohen Stuart, M. A.; Fleer, G. J. *Langmuir* **1996**, *12*, 3675.
- (27) Lowack, K.; Helm, C. A. *Macromolecules* **1998**, *31*, 823.
- (28) Decher, G.; Schmitt, J. *Prog. Colloid. Polym. Sci.* **1992**, *89*, 160.
- (29) Yoo, D.; Shiratori, S. S.; Rubner, M. F. *Macromolecules* **1998**, *31*, 1, 4309.
- (30) Roscoe, S. B.; Yitzchaik, S.; Kakkar, A. K.; Marks, T. J.; Xu, Z.; Ahang, T.; Lin, W.; Wong, G. K. *Langmuir* **1996**, *12*, 5338.
- (31) Katz, H. E.; Wilson, W. L.; Scheller, G. *J. Am. Chem. Soc.* **1994**, *116*, 6636.
- (32) Ariga, K.; Lvov, Y.; Kunitake, T. *J. Am. Chem. Soc.* **1997**, *119*, 224.
- (33) Kim, D. Y.; Li, L.; Kumar, J.; Tripathy, S. K. *Appl. Phys. Lett.* **1995**, *66*, 1166.
- (34) Todorov, T.; Nikolava, L.; Tomova, N. *Appl. Opt.* **1984**, *23*, 4309.
- (35) Wang, X.; Chen, J.-I.; Marturunkakul, S.; Li, L.; Kumar, J.; Tripathy, S. K. *Chem. Mater.* **1997**, *9*, 45.
- (36) Wang, X.; Li, L.; Chen, J.-I.; Marturunkakul, S.; Kumar, J.; Tripathy, S. K. *Macromolecules* **1997**, *30*, 219.
- (37) Shiratori, S.; Rubner, M. F. *Macromolecules* **2000**, in press.
- (38) Belletete, M.; Leclerc, M.; Durocher, G. *J. Phys. Chem.* **1994**, *98*, 9450.
- (39) Di Cesare, N.; Belletete, M.; Raymeond, F.; Leclerc, M.; Durocher, G. *J. Phys. Chem. A* **1997**, *101*, 776.
- (40) Stahelin, M.; Burland, D. M.; Ebert, M.; Miller, R. D.; Smith, B. A.; Twieg, R. J.; Volksen, W.; Walsh, C. A. *Appl. Phys. Lett.* **1992**, *61*, 1626.
- (41) Teraoka, I.; Jungbaner, D.; Reck, B.; Yoon, D. Y.; Twieg, R. J.; Willson, C. G. *J. Appl. Phys.* **1991**, *69*, 2568.
- (42) Marturunkakul, S.; Chen, J. I.; Jeng, R. J.; Sengupta, S.; Kumar, J.; Tripathy, S. K. *Chem. Mater.* **1993**, *5*, 743.
- (43) Viswanathan, N. K.; Kim, D. Y.; Bian, S.; Williams, J.; Liu, W.; Li, L.; Samuelson, L.; Kumar, J.; Tripathy, S. K. *J. Mater. Chem.* **1999**, *9*, 1941.
- (44) Kim, D. Y.; Li, L.; Jiang, X. L.; Shivshankar, V.; Kumar, J.; Tripathy, S. K. *Macromolecules* **1995**, *28*, 8835.
- (45) Bian, S.; Williams, J.; Kim, D. Y.; Li, L.; Balasubramanian, S.; Kumar, J.; Tripathy, S. K. *J. Appl. Phys.* **1999**, *86*, 4498.
- (46) Viswanathan, N. K.; Balasubramanian, S.; Li, L.; Kumar, J.; Tripathy, S. K. *J. Phys. Chem. B* **1998**, *102*, 6064.
- (47) Wang, X.; Balasubramanian, S.; Kumar, J.; Tripathy, S. K. *Chem. Mater.* **1998**, *10*, 1546.

MA9921495